第 33 卷 第 2 期 原 子 核 物 理 评 论 Vol. 33, No. 2
2016 年 6 月 Nuclear Physics Review June, 2016

Article ID: 1007-4627(2016) 02-0197-06

Revisit to Two-Proton Radioactivity of ^{19}Mg and Observation of Two-Proton Decay of ^{30}Ar

XU Xiaodong(徐晓栋)[1,2,3], I. Mukha[1,4], L. Acosta[5,6], E. Casarejos[7], A. A. Ciemny[8], W. Dominik[8], J. Duénas-Díaz[9], V. Dunin[10], J. M. Espino[11], A. Estradé[12], F. Farinon[2], H. Geissel[1,2], A. Fomichev[13], T. A. Golubkova[14], A. Gorshkov[13,15], L. V. Grigorenko[13,16,4], Z. Janas[8], G. Kamiński[17,13], O. Kiselev[2], R. Knöbel[2,1], S. Krupko[13,15], M. Kuich[18], Yu. A. Litvinov[2], G. Marquinez-Durán[9], I. Martel[9], C. Mazzocchi[8], C. Nociforo[2], A. K. Ordúz[9], M. Pfützner[8,2], S. Pietri[2], M. Pomorski[8], A. Prochazka[2], S. Rymzhanova[13], A. M. Sánchez-Benítez[9], C. Scheidenberger[1,2], P. Sharov[13], H. Simon[2], B. Sitar[19], R. Slepnev[13], M. Stanoiu[20], P. Strmen[19], I. Szarka[19], M. Takechi[2], Y. K. Tanaka[2,21], H. Weick[2], M. Winkler[2], J. S. Winfield[2]

(*1. II. Physikalisches Institut, Justus-Liebig-Universität Gießen, 35392 Gießen, Germany;*
2. GSI Helmholtzzentrum für Schwerionenforschung GmbH, 64291 Darmstadt, Germany;
3. School of Physics and Nuclear Energy Engineering, Beihang University, 100191 Beijing, China;
4. National Research Centre "Kurchatov Institute", Kurchatov sq. 1, 123182 Moscow, Russia;
5. INFN, Laboratori Nazionali del Sud, Via S. Sofía, 95123 Catania, Italy;
6. Instituto de Física, Universidad Nacional Autónoma de México, México, D.F. 01000, Mexico;
7. University of Vigo, 36310 Vigo, Spain;
8. Faculty of Physics, University of Warsaw, 02-093 Warszawa, Poland;
9. Department of Applied Physics, University of Huelva, 21071 Huelva, Spain;
10. Veksler and Baldin Laboratory of High Energy Physics, JINR, 141980 Dubna, Russia;
11. Department of Atomic, Molecular and Nuclear Physics, University of Seville, 41012 Seville, Spain;
12. University of Edinburgh, EH1 1HT Edinburgh, United Kingdom;
13. Flerov Laboratory of Nuclear Reactions, JINR, 141980 Dubna, Russia;
14. Advanced Educational and Scientific Center, Moscow State University, 121357 Moscow, Russia;
15. FSBI "SSC RF ITEP" of NCR "Kurchatov Institute", 117218 Moscow, Russia;
16. National Research Nuclear University "MEPhI", 115409 Moscow, Russia;
17. Institute of Nuclear Physics PAN, 31-342 Kraków, Poland;
18. Faculty of Physics, Warsaw University of Technology, 00-662 Warszawa, Poland;
19. Faculty of Mathematics and Physics, Comenius University, 84248 Bratislava, Slovakia;
20. IFIN-HH, Post Office Box MG-6, Bucharest, Romania;
21. University of Tokyo, 113-0033 Tokyo, Japan)

Received date: 10 Sep. 2015;

Foundation item: Helmholtz International Center for FAIR (HIC for FAIR); Helmholtz Association (IK-RU-002); Russian Ministry of Education and Science (NSh-932.2014.2); Russian Foundation for Basic Research (14-02-00090-a); Polish National Science Center (UMO-2011/01/B/ST2/01943); Polish Ministry of Science and Higher Education (0079/DIA/2014/43, Grant Diamentowy); Helmholtz-CAS Joint Research Group (HCJRG-108); FPA2009-08848 contract (MICINN, Spain)

Biography: XU Xiaodong, (1987–), male, Shangnan, Shaanxi, experimental research on nuclear structure; E-mail: X.Xu@gsi.de.

Abstract: An experiment aimed to investigate the two-proton (2p) decay of the previously unknown nucleus ^{30}Ar was performed at GSI. By tracking the decay products in-flight with silicon micro-strip detectors, the 2p decays of ^{30}Ar were observed for the first time. For the calibration purpose, 2p decays of ^{19}Mg were also remeasured by tracking the coincident ^{17}Ne+p+p trajectories. By comparing the measured angular p-^{17}Ne correlations with those obtained from the corresponding Monte Carlo simulations, the simultaneous 2p decay of ^{19}Mg ground state and the sequential 2p emission of several known excited states of ^{19}Mg were confirmed. One new excited state in ^{19}Mg and two new excited states in ^{18}Na were observed.

Key words: proton drip line; decay by proton emission; nuclear energy level

CLC number: O571 **Document code:** A **DOI:** 10.11804/NuclPhysRev.33.02.197

1 Introduction

2p radioactivity was predicted to appear in the very neutron-deficient nuclei located around the proton drip line by Goldansky in the early 1960s[1]. This exotic phenomenon is a three-body decay process resulting in a simultaneous emission of two protons. Due to the paring interaction, one-proton emission is energetically prohibited from some nuclei but the ejection of two protons is allowed. The ground-state 2p radioactivity was discovered in 2002, when it was found that the ground state (g.s.) of ^{45}Fe decays by emitting two protons simultaneously[2–3]. This exotic decay mode was also found later in ^{54}Zn[4], ^{19}Mg[5], and ^{48}Ni[6].

Among the above-mentioned g.s. 2p emitters, the lifetime of ^{45}Fe, ^{48}Ni, and ^{54}Zn is a few ms. Therefore the conventional implantation-decay method can be employed to study their decay properties. In the ^{19}Mg case, its lifetime is only a few ps. The targeted nucleus in our experiment, ^{30}Ar, was also predicted to have a very short lifetime[7]. Thus, an experimental technique applied to decays in-flight was proposed to study the radioactivity of proton-unbound nuclei in a ps-ns lifetime range[8]. This novel technique has been successfully used in the discovery of the first case of 2p radioactivity in an s-d shell nucleus ^{19}Mg[5].

2 Experiment

The search of ^{30}Ar was performed at the Fragment Separator (FRS)[9] in GSI. The FRS is a in-flight magnetic separator and spectrometer for radioactive ion beams and it consists of several dipole, quadrupole and sextupole magnets, the latter for 2nd-order correction. The layout of FRS with its several focal planes (S1 to S4) is displayed in Fig. 1. In our experiment, the primary 885 *A*MeV ^{36}Ar beam was delivered to impinge a 8 g/cm^2 primary ^{9}Be target. Then the 620 *A*MeV ^{31}Ar fragments were selected as the secondary beam and transported by the first half of FRS to bombard the secondary target (4.8 g/cm^2, ^{9}Be) located at middle focal plane S2. A 5 g/cm^2-thick Al wedge degrader was installed in the first focal plane S1 and shaped to achieve an achromatic focusing of ^{31}Ar at S2. ^{30}Ar nuclei were produced via one-neutron (1n) knockout reactions. The second half of FRS was tuned to transmit the heavy decay products, in particular ^{28}S, down to S4. For calibration purposes, the previously-known 2p radioactive nucleus ^{19}Mg was produced by 1n knockout from ^{20}Mg ions obtained by fragmenting a 685 *A*MeV ^{36}Ar beam. Its 2p decay properties were remeasured. Reactions of interest in our experiment are outlined in the lower part of Fig. 1.

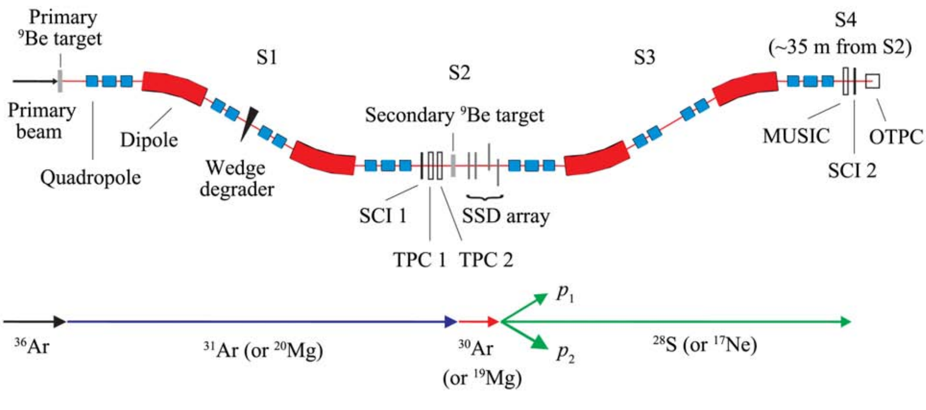

Fig. 1 (color online) Upper part: Schematic view of the experimental setup at FRS. Lower part: The reactions of interest concerning the production and decay of ^{30}Ar and ^{19}Mg.

The main detectors employed in the experiment are also sketched in Fig. 1. At S2, two Time-Projection Chambers (TPC 1 and TPC 2) were used to track the incoming ^{31}Ar (or ^{20}Mg) projectiles. Downstream from the secondary target, a silicon micro-strip detector (SSD) array which consisted of four large-area SSDs was employed to measure positions of two protons and the heavy recoil ion (^{28}S or ^{17}Ne) resulting from the in-flight 2p decay. The position measurement by SSDs allowed us to reconstruct all fragment trajectories and to derive the reaction vertex together with angular proton-proton and proton-heavy ion correlations. In the second half of FRS, the heavy-ion (HI) decay products (*i.e.*, ^{28}S or ^{17}Ne) were unambiguously identified by their magnetic rigidity ($B\rho$), time of flight (TOF) measured with two position-sensitive scintillators (SCI 1 and SCI 2), and energy loss (ΔE) in an ionization chamber (MUSIC). In addition, an optical time-projection chamber (OTPC) was installed at S4 to detect beta decays of stopped ^{31}Ar ions. Recently, the beta-delayed 3p decays of ^{31}Ar were observed and investigated[10].

2.1 Identification of decay products

The particle identification (PID) for the HI was obtained by the aforementioned $B\rho$-TOF-ΔE measurements. Fig. 2 is a two-dimensional PID plot for the ions measured at two FRS settings optimized to transmit ^{31}Ar and ^{28}S. In this plot, each nucleus sits in a unique position according to its proton number Z and mass-to-charge ratio A/Q. Therefore, the HI decay product can be identified unambiguously. Its trajectory which passed through the SSD array was measured by SSDs. The emitted protons were identified by registering its impact position in several SSD's and requiring a "straight-line" trajectory. Then the identification of a 2p decay event was performed by searching the triple HI+p+p coincidence. The meeting point of trajectories of two protons and HI is defined as the decay vertex.

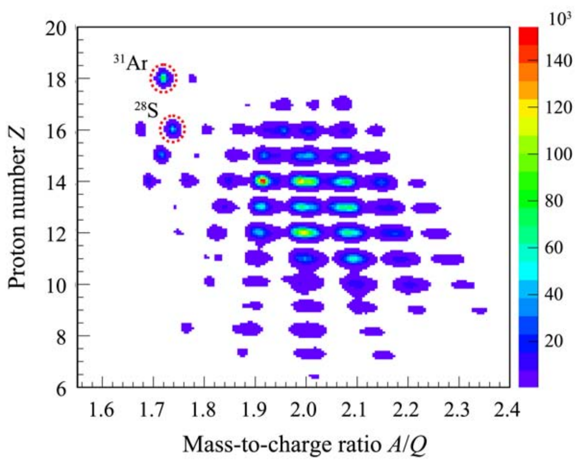

Fig. 2 (color online) Particle identification plot for ions detected at S4. The first half of FRS was optimized to transport a 620 AMeV ^{31}Ar beam and the second half of FRS was tuned to transmit the ^{28}S ions.

2.2 2p decays of ^{19}Mg

The angular correlations are similar to transverse momentum correlations which are often used to identify nuclear states and their decay channels[11]. The measured angular correlations of protons with respect to the 2p decay daughter nucleus can be employed to identify the energy levels of the 2p precursor and to deduce the decay properties (*e.g.*, decay energy and width) of the state. This method has been successfully applied in previous investigations on ^{19}Mg and ^{16}Ne[11–12]. In the same manner, we measured the angles between 2p-decay products of ^{19}Mg (and ^{30}Ar) and reconstructed the angular correlations. The present work mainly focuses on the analysis of the angular p-^{17}Ne correlations obtained from the ^{17}Ne+p+p coincidences.

Fig. 3(a) shows the scatter plot ($\theta_{^{17}\mathrm{Ne-p1}}$, $\theta_{^{17}\mathrm{Ne-p2}}$) for measured angles between protons and ^{17}Ne. There are several statistical enhancements in this angular correlation plot, which provide the information on the 2p states in ^{19}Mg and 1p levels in ^{18}Na. The angles from 2p decays of narrow states in ^{19}Mg are accumulated along arcs with radius $\rho_\theta = const$, where $\rho_\theta = \sqrt{\theta^2_{\mathrm{HI-p1}} + \theta^2_{\mathrm{HI-p2}}}$. As shown by Ref. [12], the peaks in the ρ_θ spectrum are related to ^{19}Mg resonances with the total 2p-decay energy $Q_{2\mathrm{p}} \sim \rho^2_\theta$.

In the present study, the ρ_θ distribution obtained for ^{19}Mg 2p decays is displayed in Fig. 3(b). Several intense peaks which indicate the 2p decays of various states in ^{19}Mg are clearly seen and labeled by Roman numerals. Correspondingly, the arcs shown in Fig. 3(a) are angular p-^{17}Ne correlations from the decays of these states in ^{19}Mg. The ρ_θ spectrum is very helpful to select the decay events from a certain ^{19}Mg state. In comparison with the previous data (see Fig. 2 in Ref. [12]), the angular p-^{17}Ne correlations obtained in the present work show the g.s. and several previously known excited states of ^{19}Mg. The g.s. is labeled by (i), while known excited states are marked by (ii), (iii), and (iv) respectively. In addition, the present data give hints on one unknown excited state (e.s.) of ^{19}Mg which is labeled by (v). Obviously, the new state has higher excitation energy than all known excited states.

To deduce decay properties of the observed nuclear states, detailed Monte Carlo simulations of exp-

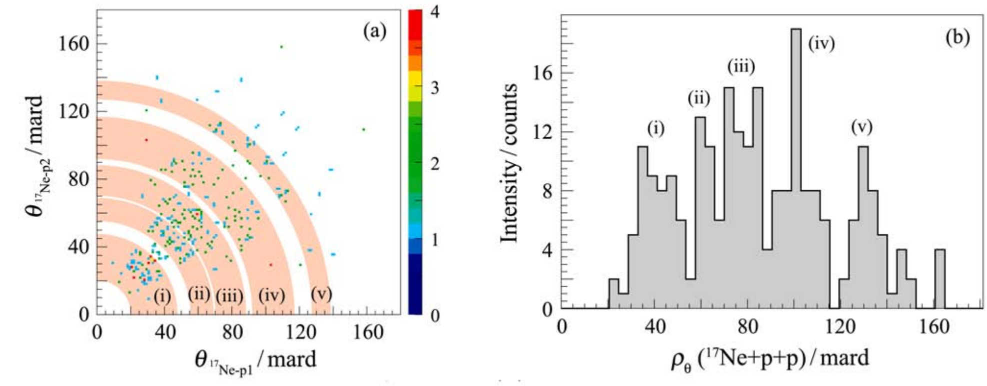

Fig. 3 (color online) Angular correlations $\theta_{^{17}\text{Ne-p1}}$-$\theta_{^{17}\text{Ne-p2}}$ (a) and ρ_θ (b) measured for the coincident ^{17}Ne+p+p events. The peaks and bands marked by "(i)-(v)" are one-to-one correspondence.

erimental response to the 2p decay of ^{19}Mg are necessary. Simulations were performed based on two decay mechanisms: a simultaneous 2p-decay mechanism[13] for the ^{19}Mg g.s. and sequential emission of protons from ^{19}Mg e.s. via ^{18}Na states. In Fig. 4(a), the Monte Carlo simulation of the simultaneous 2p decay of ^{19}Mg g.s. is compared with the experimental $\theta_{^{17}\text{Ne-p}}$ distribution obtained by selecting events in the arc-gate (i), *i.e.*, $20 < \rho_\theta < 48$ mrad. The agreement between the simulation and the data is very good. The probability that the simulated $\theta_{^{17}\text{Ne-p}}$ distribution matches experimental pattern was calculated by using a statistical Kolmogorov-Smirnov test. The stars in Fig. 4(b) displays such probability as a function of 2p decay energy $Q_{2\text{p}}$, while the solid curve is the fit of the probability distribution by a skewed Gaussian function. The highest probability corresponds to $Q_{2\text{p}} = 0.87$ MeV. The statistical uncertainty is obtained by calculating the $Q_{2\text{p}}$ range where the simulation can reproduce the data with probabilities above 50%. Thus the 2p-decay energy of ^{19}Mg g.s. derived from present work is $Q_{2\text{p}} = 0.87^{+0.16}_{-0.06}$ MeV, which is consistent with the previous data: 0.76(6) MeV[12].

Regarding the known excited states in ^{19}Mg sh-

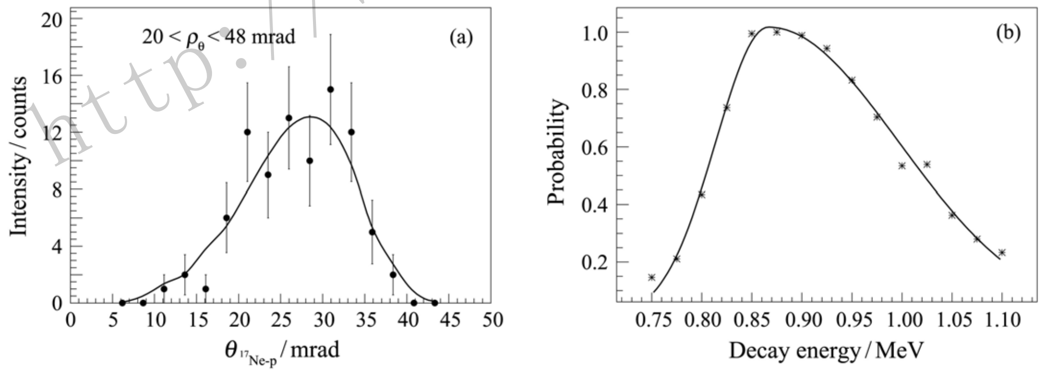

Fig. 4 (a) Measured angular p-^{17}Ne correlations (full circles with statistical errors) derived from the ^{17}Ne+p+p events with $20 < \rho_\theta < 48$ mrad, which corresponds to the ^{19}Mg g.s. region. The solid curve represents the $\theta_{^{17}\text{Ne-p}}$ distribution obtained from the simulation of detector response to the simultaneous 2p decay of ^{19}Mg g.s. with $Q_{2\text{p}} = 0.87$ MeV. (b) The resulting distribution of probability from the simulation that reproduces the data as a function of the assumed $Q_{2\text{p}}$. The curve displays the fit to the probability distribution by a skewed Gaussian function.

own by the peaks and arcs (ii), (iii), and (iv) in Fig. 3, the simulations were performed by assuming the sequential 2p decay via low-lying ^{18}Na states. The simulated $\theta_{^{17}\text{Ne-p}}$ distributions were compared with the data obtained by choosing events with the ρ_θ gates (ii), (iii), and (iv) indicated in Fig. 3(a). The corresponding results are shown in the panels (a), (b), and (c) of Fig. 5, respectively. One can clearly see the simulations generally reproduce the data. The deduced 2p-decay energies of e.s. (ii) and e.s. (iv) are: 2.1(3) and 5.3(2) MeV respectively, which agree with the previous data on the respective states at 2.14(23) and 5.5(2) MeV[12]. The determined $Q_{2\text{p}}$ for broad peak (iii) is 3.3(3) MeV, which matches the previously-measured states at 2.9(2) and 3.6(2) MeV. However, these two states cannot be resolved in the present experiment.

Evidence for one new e.s. of ^{19}Mg is shown by the peak (v) in Fig. 3(b). One can see that most events

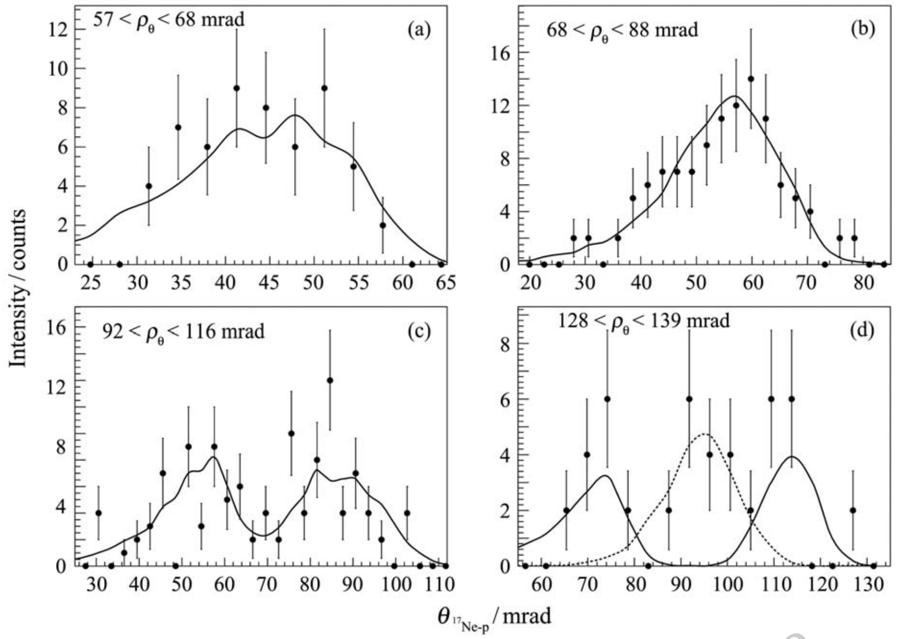

Fig. 5　Same as Fig. 4(a) but for the excited states of ^{19}Mg. (a) The 2p decay of e.s. gated by (ii), $57 < \rho_\theta < 68$ mrad. The curve displays the simulation of the sequential 2p decay of ^{19}Mg state at 2.1 MeV via ^{18}Na state at 1.23 and 1.55 MeV. (b) The 2p decays gated by (iii), $68 < \rho_\theta < 88$ mrad. The solid curve is the simulation of the sequential 2p decay of ^{19}Mg state at 3.3 MeV state via the 1.55 and 2.084 MeV levels of ^{18}Na. (c) The 2p decays gated by (iv), $92 < \rho_\theta < 116$ mrad. The result of the simulation to the sequential 2p emission of ^{19}Mg state at 5.3 MeV via 1.55 MeV state of ^{18}Na state is depicted by the solid curve. (d) The 2p decay of new discovered e.s. in ^{19}Mg gated by (v), $128 < \rho_\theta < 139$ mrad. The solid curve and dashed curve are the $\theta_{^{17}\mathrm{Ne-p}}$ distribution obtained by simulation of 2p emission of ^{19}Mg state at 8.8 MeV via two new observed ^{18}Na states at 2.6 and 4.1 MeV, respectively.

within the corresponding band (v) in Fig. 3(a) fall into four clusters which indicate sequential emission of protons from one e.s. of ^{19}Mg via two states of ^{18}Na. Because such a structure cannot be described by sequential 2p decay via any previously-known ^{18}Na state, the existence of two new ^{18}Na levels has to be assumed. To verify the assumption, we performed Monte Carlo simulations. By properly adjusting the decay energies and lifetimes of the ^{19}Mg state and two ^{18}Na levels, it was found that the simulation of sequential emission of protons from ^{19}Mg e.s. at 8.8 MeV via the excited states of ^{18}Na at 2.6 and 4.1 MeV can describe the data reasonably. The corresponding simulations are displayed by the solid and dashed curves in Fig. 5(d), respectively. It is worth noting that Fortune has predicted the energy level of ^{18}Na at 2.6 MeV[14].

2.3　2p decays of ^{30}Ar

Following a similar procedure to that conducted for 2p decays of ^{19}Mg, we identified 2p decays of ^{30}Ar by measuring the coincident ^{28}S+p+p trajectories. The decay vertex and fragment correlations were reconstructed. Fig. 6(a) shows the scatter plot of $\theta_{^{28}\mathrm{S-p1}}$ versus $\theta_{^{28}\mathrm{S-p2}}$ for measured ^{28}S+p+p coinci-

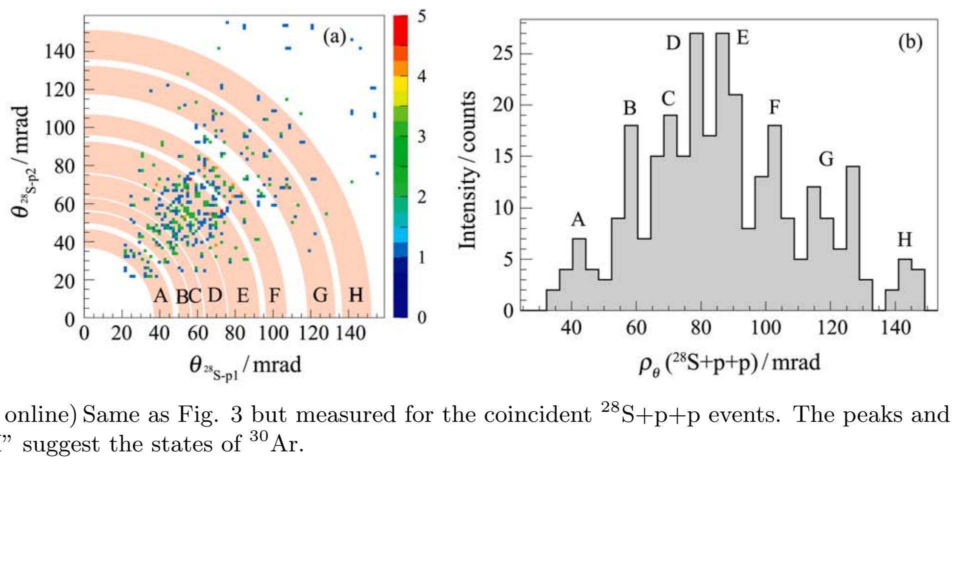

Fig. 6　(color online) Same as Fig. 3 but measured for the coincident ^{28}S+p+p events. The peaks and bands labeled by "A-H" suggest the states of ^{30}Ar.

dences. The statistical enhancements observed in the figure indicate the ^{30}Ar decays. The corresponding ρ_θ values were calculated and their distribution is plotted in Fig. 6(b). Several peaks are clearly observed and labeled by uppercase letters. The bands in Fig. 6(a) and the peaks in Fig. 6(b) are one-to-one correspondence. These bands and peaks demonstrate the observation of 2p decays from several states of ^{30}Ar. The detailed study concerning the structure of several low-lying states in unknown nucleus ^{30}Ar and ^{29}Cl can be found in Ref. [15].

3 Summary

An experimental investigation on the 2p decays of ^{19}Mg and unknown nucleus ^{30}Ar is reported. The 2p-decay energies of ^{19}Mg both for g.s. and for known excited states are confirmed. Moreover, we observed a new excited state in ^{19}Mg and we found it decays by emitting two protons via two new excited states in ^{18}Na. We also investigated the unknown nucleus ^{30}Ar and observed its 2p decays for the first time.

Acknowledgments This work was supported in part by Helmholtz International Center for FAIR (HIC for FAIR), the Helmholtz Association (grant IK-RU-002), the Russian Ministry of Education and Science (grant No. NSh-932.2014.2), the Russian Foundation for Basic Research (grant No. 14-02-00090-a), the Polish National Science Center (Contract No. UMO-2011/01/B/ST2/01943), the Polish Ministry of Science and Higher Education (Grant No. 0079/DIA/2014/43, Grant Diamentowy), the Helmholtz-CAS Joint Research Group (grant HCJRG-108), the FPA2009-08848 contract (MICINN, Spain). Authors declare that this article is a part of Ph.D. work of XU Xiaodong.

References:

[1] GOLDANSKY V I. Nucl Phys, 1960, **19**: 482.
[2] PFÜTZNER M, BADURA E, BINGHAM C, *et al.* Eur Phys J A, 2002, **14**: 279.
[3] GIOVINAZZO J, BLANK B, CHARTIER M, *et al.* Phys Rev Lett, 2002, **89**: 102501.
[4] BLANK B, BEY A, CANCHEL G, *et al.* Phys Rev Lett, 2005, **94**: 232501.
[5] MUKHA I, SÜMMERER K, ACOSTA L, *et al.* Phys Rev Lett, 2007, **89**: 182501.
[6] POMORSKI M, PFÜTZNER M, DOMINIK W, *et al.* Phys Rev C, 2011, **83**: 061303.
[7] GRIGORENKO L V, ZHUKOV M V. Phys Rev C, 2003, **68**: 054005.
[8] MUKHA I, SCHRIEDER G. Nucl Phys A, 2001, **690**: 280.
[9] GEISSEL H, ARMBRUSTER P, BEHR K H, *et al.* Nucl Inst Meth B, 1992, **70**: 286.
[10] LIS A A, MAZZOCCHI C, DOMINIK W, *et al.* Phys Rev C, 2015, **91**: 064309.
[11] MUKHA I, SÜMMERER K, ACOSTA L, *et al.* Phys Rev C, 2010, **82**: 054315.
[12] MUKHA I, GRIGORENKO L, ACOSTA L, *et al.* Phys Rev C, 2012, **85**: 044325.
[13] GRIGORENKO L V, MUKHA I G, ZHUKOV M V. Nucl Phys A, 2003, **713**: 372; **740**: 401(E), 2004.
[14] FORTUNE H T, SHERR R. Phys Rev C, 2007, **76**: 014313.
[15] MUKHA I, GRIGORENKO L V, XU X, *et al.* Phys Rev Lett, 2015, **115**: 202501.